

Rethinking Classification Loss Designs for Person Re-identification with a Unified View

Zhizheng Zhang¹ * Cuiling Lan² Wenjun Zeng² Zhibo Chen¹ Shih-Fu Chang³

¹ University of Science and Technology of China

² MicroSoft Research Asia

³ Columbia University

zhizheng@mail.ustc.edu.cn, {culan, wezeng}@microsoft.com,
chenzhibo@ustc.edu.cn, sc250@columbia.edu

Abstract. Person Re-identification (ReID) aims at matching a person of interest across images. In convolutional neural networks (CNNs) based approaches, loss design plays a role of metric learning which guides the feature learning process to pull closer features of the same identity and to push far apart features of different identities. In recent years, the combination of classification loss and triplet loss achieves superior performance and is predominant in ReID. In this paper, we rethink these loss functions within a generalized formulation and argue that triplet-based optimization can be viewed as a two-class subsampling classification, which performs classification over two sampled categories based on instance similarities. Furthermore, we present a case study which demonstrates that increasing the number of simultaneously considered instance classes significantly improves the ReID performance, since it is aligned better with the ReID test/inference process. With the multi-class subsampling classification incorporated, we provide a strong baseline which achieves the state-of-the-art performance on the benchmark person ReID datasets. Finally, we propose a new meta prototypical N-tuple loss for more efficient multi-class subsampling classification. We aim to inspire more new loss designs in the person ReID field.

Keywords: Person re-identification, Loss design, Retrieval, Classification

1 Introduction

Person re-identification (ReID) aims to identify the same persons across images captured at different times, or places, or from different cameras. This is an attractive task for both academia and industry. The objective of CNN-based person ReID methods is to minimize the feature discrepancy (distances) among the samples with the same identity while maximizing the feature discrepancy (distances) among the samples of different identities in the embedding space to encourage the separation between positive sample pairs and negative sample pairs.

Person ReID lies in between image classification [19,63] and instance retrieval [62], where the image classes (identities) are available during training while the identities of a query image are previously “unseen” [61] in the testing/inference. ReID inference

* This work was done when Zhizheng Zhang was a visiting student at Columbia University.

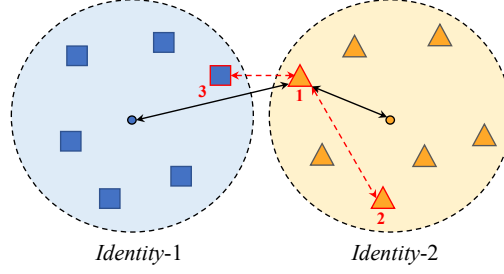


Fig. 1. A toy example of samples with different identities in the embedding space.

can be considered as a retrieval process. Given a query image, its distances (or similarity) to all the samples in the gallery set will be calculated and ranked to identify the matched images. In the early stage, there have been debates in this field on whether triplet loss or classification loss is more suitable for this task. Many researchers stand up in defense of triplet loss or its variants for training CNN-based person ReID models [29,6,13,69,54,2,55]. Given a person sample as the anchor, triplet-based loss optimizes its distance to the samples (or the centroids of several samples) with the same identity to be closer than its distance to the samples (or the centroids of several samples) with a different identities. At the same time, there are many works [22,41,53,56] that use conventional classification loss for feature learning, by treating ReID as a classification problem over all identities in the training set (with each identity taken as a category). Recently, many state-of-the-art works [48,57,58,20,27] combine both triplet loss and classification loss, which leads to superior performance than using only one of them.

Fig. 1 illustrates the roles triplet loss and classification loss play in optimization. Traditional classification loss enforces global-scope optimization which pushes for the separation of class centers but does not ensure the reasonableness of the relative order of the distances among sample pairs. For example, the distance between sample-1 and sample-2 (of the same identity) is even larger than the distance between sample-1 and sample-3 (of different identities). Triplet loss guides the feature learning in a local manner, *i.e.*, from triple instances, to optimize the relative orders of the distances of two sample pairs. As shown in Fig. 1, a triplet consists of an anchor (*e.g.* sample-1), a positive sample that has the same identity as the anchor (*e.g.* sample-2), and a negative sample with different identity (*e.g.* sample-3). The triplet loss aims to reduce the distance (d_{12}) of the positive pair and enlarge the distance of the negative pair (d_{13}) to make d_{13} be larger than d_{12} by a margin in the embedding space. Both global-scope optimization and local instance-level optimization are valuable for ReID. Most researches focus on these two extremes for person ReID. There is a lack of more comprehensive study on the effectiveness of losses at multiple granularities.

In this paper, we rethink the loss designs for person ReID and reformulate the losses in a unified classification view. The popular losses like triplet loss, classification loss can be formulated in a generalized form. From the reformulation, triple loss with soft margin can be considered as a two-class subsampling classification wherein we consider the anchor (*e.g.* sample-1) as the sample to be classified while taking the other sam-

pled instances (*e.g.* sample-2 and sample-3) as the non-parametric weight vectors for classification. The conventional classification loss treats each identity as a class and the parameters of the classifier weight vectors of a Fully Connected (FC) layer) play the role of “class centers”. Thus, an anchor sample is “compared” with all the “class centers” to identify its class in training. We argue that two-class subsampling classification as a local constraint is too local to be optimal and the consideration of the more general *multi-class* subsampling classification as a mid-level constraint can significantly enhance the quality of embedding and the ReID performance. This benefits from the joint comparison with multi-class instances which better matches the nature of ReID inference, *i.e.*, distance ordering across many images in the gallery set. We validate the effectiveness of the multi-class subsampling classification loss on several benchmark datasets. Moreover, we propose a new meta prototypical N-tuple (MPN-tuple) loss for more efficient multi-class subsampling classification, which enables a more general similarity metric and reduces the number of packaged N-tuplets.

We summarize our main contributions as follows:

- We revisit the prevalent losses in person ReID and encompass them under a unified mathematical formulation.
- We conduct a systematic empirical study with both triplet loss and conventional classification loss and provide a strong baseline by revisiting the design choices and their combination.
- We take a further step to study the good practice of the combined use of two-class subsampling classification, multi-class subsampling classification, and conventional classification. This provides flexibility and a hierarchy of optimization at different granularities, *i.e.*, local level, mid-level, and global level.
- We propose a new loss, meta prototypical N-tuple (MPN-tuple) loss, for multi-class subsampling classification.

While simple, our scheme achieves the state-of-the-art performance, outperforming that of previous loss designs by a large margin. We will release our source code once accepted. We hope that our scheme could serve as a new strong baseline which benefits the ReID community.

2 Related Works

2.1 Person Re-identification

Person ReID aims to learn discriminative feature representations which are capable of identifying the same person while distinguishing different persons based on feature distance (or similarity) comparison. The inference of person ReID is to rank the gallery images by comparing their feature distances to the query image. Many efforts have been made for representative feature learning from the network or loss design perspectives.

For person ReID, deep learning based approaches have significantly outperformed conventional approaches which use hand-crafted features [31,64,24,39]. Some approaches exploit multi-granularity feature representation to capture both global and local features for ReID [3,48,22,51,38,59,28]. Some others introduce attention mechanisms for discriminative feature learning, which aim to strengthen the discriminative features while

suppressing the irrelevant ones [23,45,58,4,37]. To tackle the challenges of diverse viewpoints and poses, many works exploit some auxiliary semantics (*e.g.* segmentation [37], parsing [17], pose [38,59], dense semantics [57,16]) to address the misalignment in person ReID.

In addition to network designs, loss designs also play an important role in person ReID, which influence the quality of the learned features. In the early years, some works employ the contrastive loss [42,43,46] and verification loss [21,1] to optimize person ReID networks. By introducing relative distance order between the positive sample pair and the negative sample pair, triplet loss and its variants prevail [18,29,6,13,69,54,2,55] for person ReID. Hermans *et al.* introduce a batch-level hard triplet mining which selects the hardest positive and the hardest negative samples within that batch when forming the triplets for computing the loss [13]. Besides, soft-margin shows superiority to hard margin. Some works introduce the centroids of several samples in the triplet construction and perform optimization towards the upper bound of the triplet loss [69,54,55]. Chen *et al.* propose the quadruplet loss which is built based on triplet loss and additionally pushes away negative pairs from positive pairs w.r.t different probe images [5]. These losses belong to local optimization which only jointly optimizes three to four samples. As a remedy, conventional classification loss with trainable fully connected layer for identity classification is widely used for feature learning in ReID [22,41,53,56], in which each identity corresponds to a category. Most of the recent works combine triplet-based loss and conventional classification loss for higher performance [48,57,58,9,20,27].

2.2 Metric Learning

The study on metric learning [34,52] stemmed from the era before the deep learning and it has been an indispensable part of deep learning in the form of loss design for many applications, such as person ReID [43,13,5], vehicle ReID [26], few-shot learning [44,35]. As one of the most commonly used pairwise losses, the contrastive loss is investigated in [10]. Triplet-based losses setup an anchor and pull the distance between positive pair to be smaller than the negative pair. To guarantee the effectiveness of selected triplets, batch hard mining [13] and the use of soft margin [13,20] are widely used. Triplet loss is also improved in its speed and robustness by generalizing from optimizing instance-to-instance distances to optimizing instance-to-centroid distances towards its upper bound [8]. $(N + 1)$ -tuple loss pushes $N - 1$ negative samples and pull the positive pair *all at once* [36]. Conceptually interesting, however, such joint ordering of multiple classes is under-explored in ReID.

In this paper, we revisit loss designs for person ReID and reformulate the losses from a unified classification view, although they differ in the classifier construction and optimization scope. Moreover, we raise an overlooked issue in current loss designs in ReID and highlight that multi-class submapping classification has an important impact on model performance, hopefully enabling other researchers in the field to leverage the full potential of multi-class joint optimization.

3 Revisiting Loss Designs for Person ReID Under a Unified View

In this section, we reformulate the losses from a unified classification view and revisit the commonly used loss designs for person ReID. We show that the triplet loss can be treated as optimizing a two-class subsampling classification while conventional classification corresponds to a full-class classification under this formulation. We further point out that increasing the number of classes in subsampling classification is important but overlooked in the current practice of loss designs in person ReID community.

Moreover, we propose a Meta Prototypical N-tuple (MPN-tuple) loss for more efficient multi-class subsampling classification. With the proposed MPN-tuple loss adopted, our scheme can serve as a strong baseline and allow a plain model to outperform the current state-of-the-arts significantly.

3.1 A Unified Loss Formulation

We formulate the loss designs from a unified classification view as:

$$\mathcal{L}_{unified} = -\log \frac{\exp(\frac{1}{\tau} \mathcal{S}(\mathbf{x}_a, \mathbf{f}_j))}{\sum_{k=1}^C \exp(\frac{1}{\tau} \mathcal{S}(\mathbf{x}_a, \mathbf{f}_k))} = \log \left(1 + \frac{\sum_{k \neq j}^C \exp(\frac{1}{\tau} \mathcal{S}(\mathbf{x}_a, \mathbf{f}_k))}{\exp(\frac{1}{\tau} \mathcal{S}(\mathbf{x}_a, \mathbf{f}_j))} \right), \quad (1)$$

where $\mathcal{S}(\cdot, \cdot)$ denotes the similarity between the two feature vectors/nodes, $\mathbf{x}_a \in \mathbb{R}^d$ denotes the feature vector (of d dimensions) of an anchor sample a to be classified/matched and $\mathbf{f}_i \in \mathbb{R}^d$ denotes a weight vector of the classifier. We can write the weight matrix as $\mathbf{W}_b = [\mathbf{f}_1, \mathbf{f}_2, \dots, \mathbf{f}_C] \in \mathbb{R}^{d \times C}$. Generally, \mathbf{f}_j with $j = 1, 2, \dots, C$ can be considered as the *reference nodes* for classification/matching. C denotes the number of the reference classes or instances. The more similar between \mathbf{x}_a and a reference \mathbf{f}_j , the higher of the probability that they belong to the same class. Softmax function plays the role of normalization and it also facilitates the relative comparisons with respect to these reference nodes. τ denotes a temperature parameter. In general, the similarity function $\mathcal{S}(\cdot, \cdot)$ is often modeled by cosine similarity $\mathcal{S}(\mathbf{x}_a, \mathbf{f}_j) = (\mathbf{f}_j^T \mathbf{x}_a) / (\|\mathbf{x}_a\| \|\mathbf{f}_j\|)$ or the negative of Euclidean distance $\mathcal{S}(\mathbf{x}_a, \mathbf{f}_j) = -\|\mathbf{x}_a - \mathbf{f}_j\|$.

Interestingly, the unified classification formulation can degrade to different popular loss designs or evolve to new losses. They can be categorized from two perspectives: (1) what the reference nodes are instantiated to, and (2) how many classes are involved. Actually, a reference node can be implemented by gradient-optimized weight vector, or an instance feature, or an average (prototype) of multiple instance features. Taking \mathbf{x}_a as the feature of an instance, it then corresponds to the optimization of instance-to-center (global center) similarities (or distances), instance-to-instance similarities (or distances), instance-to-prototype (local center) similarities (or distances). Moreover, we can perform classification/matching over several sampled classes or over all the classes in the training set, which we refer to as **subsampling classification** and **conventional (full-class) classification** accordingly. We discuss some popular instantiations and their connections to the concept of classification. We hope our analysis from this unified view could inspire more new loss designs for person ReID.

Relation to Conventional Classification Loss. When the weight matrix $\mathbf{W}_b = [\mathbf{f}_1, \mathbf{f}_2, \dots, \mathbf{f}_C] \in \mathbb{R}^{d \times C}$ in the unified formulation is from the learned weights of a

Fully-Connected (FC) layer and $\mathcal{S}(\cdot, \cdot)$ is calculated by the inner product, the loss for the sample \mathbf{x}_a becomes the conventional classification loss as

$$\mathcal{L}_{classi} = -\log \frac{\exp(\frac{1}{\tau} \mathbf{f}_j^T \mathbf{x}_a)}{\sum_{k=1}^C \exp(\frac{1}{\tau} \mathbf{f}_k^T \mathbf{x}_a)}, \quad (2)$$

which denotes the negative logarithm of the probability of belonging to the j^{th} class for sample \mathbf{x}_a . C is the total number of categories/identities in the training set. Each reference node \mathbf{f}_k , which is implemented by a learned weight vector (parameters), plays a role of “class center”. The probability of belonging to the j^{th} class is obtained by comparing the similarities with all the “class centers”. Note that the reference nodes of the conventional classification are parameter-based and each class corresponds to one reference node. It globally optimizes the instance-to-center similarities.

However, such conventional full-class classification does not align well with the retrieval purpose of person ReID. As illustrated in Fig. 1, all samples could be correctly classified to their classes/identities based on the similarity to the two class centers. However, ReID is an open set problem (the identities in testing are unseen in training) and the inference is a retrieval process. Given sample-1 as the query image, distance-based ranking leads to a wrong ranking results of sample-2 and sample-3. Conventional classification loss is capable of enforcing global constraint but lacks the capability of optimizing the relative order of instance pairs.

Relation to Triplet Loss. Triplet loss aims at optimizing the relative order of instance pairs. The vanilla version of triplet loss encourages the similarity between the anchor and a positive sample to be larger than the similarity between this anchor and a negative sample by a hard margin m as below:

$$\mathcal{L}_{triplet} = [m + \mathcal{S}(\mathbf{x}_a, \mathbf{x}^-) - \mathcal{S}(\mathbf{x}_a, \mathbf{x}^+)]_+, \quad (3)$$

where $[\cdot]_+ = \max(\cdot, 0)$, \mathbf{x}_a , \mathbf{x}^+ , and \mathbf{x}^- denote the sampled anchor sample, the positive sample (that has same identity from \mathbf{x}_a), and the negative sample (that has different identity as \mathbf{x}_a), respectively. In the field of person ReID, the soft margin variant of triplet loss has been demonstrated to be more effective [13,20]. It replaces the hinge function $[m + \cdot]_+$ by softplus function $\log(1 + \exp(\cdot))$ which decays exponentially instead of having a hard cut off. It is defined as:

$$\mathcal{L}_{triplet} = \log(1 + \exp(\mathcal{S}(\mathbf{x}_a, \mathbf{x}^-) - \mathcal{S}(\mathbf{x}_a, \mathbf{x}^+))), \quad (4)$$

which is equivalent to:

$$\begin{aligned} \mathcal{L}_{triplet} &= \log(1 + \exp(\mathcal{S}(\mathbf{x}_a, \mathbf{x}^-)/\exp(\mathcal{S}(\mathbf{x}_a, \mathbf{x}^+))) \\ &= -\log \frac{\exp(\mathcal{S}(\mathbf{x}_a, \mathbf{x}^+))}{\exp(\mathcal{S}(\mathbf{x}_a, \mathbf{x}^+)) + \exp(\mathcal{S}(\mathbf{x}_a, \mathbf{x}^-))}. \end{aligned} \quad (5)$$

Comparing (2) and (5), we can observe that triplet loss with soft margin is actually an instantiation of the unified classification loss of (2) by setting $C = 2$, and taking the positive sample \mathbf{x}^+ and the negative sample \mathbf{x}^- as the reference nodes. The loss can be treated as the evaluation of the probability of the sample \mathbf{x}_a having the same class

as the positive sample \mathbf{x}^+ . We thus view the soft-margin triplet loss as a classification loss over two sampled categories/identities, which is also referred to as two-class subsampling classification. This loss is based on two-class subsampling and optimizes instance-to-instance distances with two instances as reference nodes. This is extremely local which only simultaneously considers three instances/samples from two classes. Note that we can adjust the range of similarity by multiplying a factor $1/\tau$ over the similarity function.

Batch Hard triplet loss [13] proposes a sampling strategy to obtain the two reference nodes. A batch-level hard mining is performed by selecting the farthest positive sample \mathbf{x}^+ relative to the anchor \mathbf{x}_a and the closest negative sample \mathbf{x}^- relative to \mathbf{x}_a as the reference nodes. Besides, some variants such as *point-to-set* triplet losses [69,54,8,55] can also be cast into our unified formulation by taking the average feature of several samples instead of one sample as the reference node. With these *point-to-set* triplet losses optimizing instance-to-prototype (local center) similarities (or distances), they still belong to 2-class subsampling classification which optimizes feature embedding in a local manner.

In the person ReID community, the joint use of triplet loss and the conventional classification loss provides superior performance and is predominant. However, this conventional classification loss does not consider the relative order of the distances of instance pairs and therefore does not well match the retrieval purpose of ReID. Triplet loss considers the relative order of distances but only simultaneously handles three instances from two classes and is thus too local. We propose that the simultaneous consideration of instances from more classes are necessary for effective person ReID. We therefore introduce the multi-class subsampling classification loss, *i.e.*, N-tuplet loss [36], to ReID.

Relation to N-tuplet Loss. N-tuplet loss [36] allows the interaction of the anchor with more than one samples from multiple different classes simultaneously, which actually corresponds to a multi-class subsampling process. Its joint optimization of multi-classes promotes the relative order of distances among more instance pairs which matches ReID retrieval well. However, it is under-explored in ReID. Consistent with the unified classification formulation, given an anchor sample \mathbf{x}_a , we rewrite it as

$$\mathcal{L}_{N\text{-tuplet}} = -\log \frac{\exp(\frac{1}{\tau}\mathcal{S}(\mathbf{x}_a, \mathbf{x}^+))}{\exp(\frac{1}{\tau}\mathcal{S}(\mathbf{x}_a, \mathbf{x}^+)) + \sum_{k=1}^{N-1} \exp(\frac{1}{\tau}\mathcal{S}(\mathbf{x}_a, \mathbf{x}_k^-))}, \quad (6)$$

where \mathbf{x}_k^- , $k = 1, \dots, N-1$ corresponds to $N-1$ negative samples of $N-1$ different classes, and \mathbf{x}^+ corresponds to a positive sample (same identity as the anchor sample). Compared to the soft-margin triplet in (5), the difference is that multiple negative samples instead of one is used in N-tuplet loss. When $N = 2$, it degrades to soft-margin triplet loss. The N-tuplet loss is based on multi-class subsampling and optimizes instance-to-instance distances with N instances as reference nodes. This is a mid-level optimization which simultaneously considers N instances/samples of N classes. In the experiment section, we demonstrate its high efficiency for person ReID.

3.2 Proposed Meta Prototypical N-tuplet Loss

In this section, based on multi-class subsampling classification loss, *i.e.*, N-tuplet loss, we propose a *Meta Prototypical N-tuplet* loss (MPN-tuplet loss) for effective person ReID. First, we enable a more general similarity metric. Second, to reduce the number of N-tuplets to make it be trackable especially when N is large, we average the samples of the same identity in the embedding space to be the class-specific prototypes within a batch, which are taken as the reference nodes for subsampling classification.

Particularly, instead of directly using the features of sampled instances as the reference nodes (as in N-tuplet loss), motivated by few shot learning [32], we add a mapping subnet $\phi(\cdot)$ as a meta learner for obtaining the reference nodes based on these instance features. We define $\phi(\mathbf{x}_k)$ as

$$\phi(\mathbf{x}_k) = W_2(\text{BN}(W_1(\mathbf{x}_k))), \quad (7)$$

where $\phi(\cdot)$ is implemented by two Fully-Connected (FC) layers with a Batch Normalization (BN), $W_1 \in \mathbb{R}^{\frac{d}{s} \times d}$, $W_2 \in \mathbb{R}^{d \times \frac{d}{s}}$, wherein s is an integer which controls the dimension reduction ratio and we set it to 8. Here, we define the similarity function \mathcal{S} as the cosine similarity of the two input vectors as

$$\mathcal{S}(\mathbf{x}_a, \phi(\mathbf{x}_k)) = (\phi(\mathbf{x}_k)^T \mathbf{x}_a) / (\|\phi(\mathbf{x}_k)\| \cdot \|\mathbf{x}_a\|). \quad (8)$$

Essentially, the introduction of ϕ enables a *more general similarity metric* between the instances, which facilitates the capture of correlations between different dimensions. For an anchor sample \mathbf{x}_a , we define the Meta N-tuplet loss as:

$$\mathcal{L}_{MN-tuple} = -\log \frac{\exp(\frac{1}{\tau} \mathcal{S}(\mathbf{x}_a, \phi(\mathbf{x}^+)))}{\exp(\frac{1}{\tau} \mathcal{S}(\mathbf{x}_a, \phi(\mathbf{x}^+))) + \sum_{k=1}^{N-1} \exp(\frac{1}{\tau} \mathcal{S}(\mathbf{x}_a, \phi(\mathbf{x}_k^-)))}. \quad (9)$$

For K samples $(\mathbf{x}_{c,j})$, with $j = 1, \dots, K$ of the class c , we build its prototype reference node by averaging their mapped features as $\widehat{\phi}_c = \frac{1}{K} \sum_{j=1}^K \phi(\mathbf{x}_{c,j})$. For an anchor sample \mathbf{x}_a , we define the Meta Prototypical N-tuple loss as

$$\mathcal{L}_{MPN-tuple} = -\log \frac{\exp(\frac{1}{\tau} \mathcal{S}(\mathbf{x}_a, \widehat{\phi}^+))}{\exp(\frac{1}{\tau} \mathcal{S}(\mathbf{x}_a, \widehat{\phi}^+)) + \sum_{k=1}^{N-1} \exp(\frac{1}{\tau} \mathcal{S}(\mathbf{x}_a, \widehat{\phi}_k^-))}, \quad (10)$$

where $\widehat{\phi}^+$ denotes the prototype reference node obtained from the positive samples (same class as the anchor sample) while $\widehat{\phi}_k^-$ denotes that for the k^{th} negative class. We will demonstrate the effectiveness of the proposed MPN-tuple loss for person ReID in the experiment section.

Discussion. All these loss designs are instantiations of our unified classification formulation. Table 1 summarizes their differences from two main aspects.

First, they differ in the number of classes/identities that are simultaneously/jointly optimized in the loss. Triplet loss (*e.g.*, triplet, batch hard mining triplet, point-to-set triplet) only uses instances from two classes for the joint optimization (see (5)) which is

Table 1. Comparisons among the different instantiations of the unified formulation of person ReID losses. Based on the definition/assignment of reference nodes (ref. nodes), there are three different optimization methods, *i.e.*, “instances to instances (Ins. to Ins.)”, “instances to prototypes (Ins. to Pro.)” and “instances to centers (Ins. to Cen.)”. Here, *prototype* refers to the local center (average) of several sampled instances while *center* refers to the globally learned class center (for each class). *Full Cls.* refers to the conventional classification over all classes. *Num. of classes* denotes the number of jointly considered classes.

	Triplet	BH Triplet	P2S Triplet	N-tuplet	MPN-tuplet	Full Cls.
Num. of classes	2	2	2	≥ 2	≥ 2	all
Optimization	Ins. to Ins.	Ins. to Ins.	Ins. to Pro.	Ins. to Ins.	Ins. to Pro.	Ins. to Cen.
Ref. nodes	features	features	features	features	learned features	parameters

a two-class subsampling classification. N-tuplet and our proposed MPN-tuple losses extend the joint optimization of two classes to multiple classes. The conventional classification loss jointly considers all the classes in the loss where each class’s reference node is represented by a learned weight vector. The joint optimization of multiple classes (as in N-tuplet in (6) and our proposed MPN-tuple losses in (10)) enables the simultaneous comparisons between the anchor sample x_a and multiple samples which come from multiple classes. In comparison with triplet loss which only involves the comparison between two classes, this multi-class mechanism aligns with the purpose of ReID inference better.

Second, they differ in the definition/assignment of reference nodes. For conventional classification, the learned parameters (weight vectors) play a role of “class centers” and are taken as the reference nodes for comparisons. For triplet and N-tuplet losses, sample instances are taken as reference nodes. We use *center* to denote the learned “class center” and use *prototype* to denote the local average of several sampled instances. Accordingly, there are three different optimization methods in calculating the similarity, *i.e.*, “instances to instances (Ins. to Ins.)”, “instances to prototypes (Ins. to Pro.)” and “instances to centers (Ins. to Cen.)”. “instances to instances” matching (similarity calculation) is consistent with the instance matching between a query image and a gallery image in ReID inference. “instances to centers” facilitates the capture of global distributions and benefits the global optimization but is less effective in serving the relative ordering between instance pairs (see explanations about Fig. 1). Thus, they are complementary. “instances to prototypes” is similar to “instances to instances”. The local average of several sampled instances (of the same class) to form a prototype is expected to provide a reference node being robust to outliers and provide a way to reduce the number of triplets/tuplets within a batch.

4 Experiments

4.1 Datasets and Evaluation Metrics

To investigate the effectiveness of different loss designs, we conduct experiments on four public person ReID datasets.

CUHK03 [21] consists of 1,467 pedestrians from six non-overlapped cameras. This dataset provides both manually labeled bounding boxes and DPM-detected bounding boxes from 14,097 images. The new training/testing protocol of [67,12] is used where 767 identities are used for training. We only show the evaluation results for the labeled setting (L) while the detected setting (D) presents a similar trend.

Market1501 [60] consists of 1,501 identities with 751 for training and the rest for testing. It has 12,936 training images, 3,368 query images and 19,732 gallery images.

DukeMTMC-reID [66] is a subset of Duke Dataset [33]. The standard training/testing split and evaluation setting as used in [66,25] are adopted. It consists of 16,522 training images of 702 identities, 2,228 query images of the other 702 identities and 17,661 gallery images.

MSMT17 [50] is a newly released large dataset which consists of 4101 identities from 15 cameras (including 12 outdoor cameras and 3 indoor cameras). It provides a total of 126441 images with different weather conditions when collecting them and with bounding boxes annotated.

Evaluation Metrics. We follow the common practices and use the cumulative matching characteristics (CMC) at Rank-1 and mean average precision (mAP) to evaluate the performance.

4.2 Implementation Details

Network Settings. We follow the common practices in ReID [2,57,27] and take ResNet-50 [11] to build our baseline network for effectiveness validation. Similar to [40,57], we remove the last spatial down-sampling operation in the conv5_x block of ResNet-50. Similar to [30], we add Instance Normalization to the first three blocks (conv2_x-conv4_x) to enhance model’s generalization ability [15], which is found effective in improving the performance because the identities during testing are unseen (different from the training identities). All our studies are based on this improved ResNet-50. More details can be found in the Supplementary. On top of the spatially pooled feature (2048 dimensions) of ResNet-50, a Batch Normalization (BN) layer is added to obtain the ReID feature vector $\mathbf{x} \in \mathbb{R}^{1024}$ and a followed Fully Connected (FC) layer is employed as the classifier for adding the conventional classification loss. In our studies, the subsampling classification losses are added on the ReID feature vector \mathbf{x} by default. Note that we do not implement re-ranking [67] in all our experiments.

For each loss, to automatically choose a suitable temperature parameter τ , similar to [47], we implement this by using a learnable network parameter τ and it is automatically learned by gradients back-propagation instead of introducing a new hyper-parameter.

Training. We use the commonly used data augmentation strategies of random cropping [49], horizontal flipping, and random erasing [49,45]. The input resolution is set to 384×128 for all the datasets. The backbone network is pre-trained on ImageNet[7]. We adopt Adam optimizer to train all models. Please see Supplementary for more details.

Each batch includes $B = P \times K$ images. P and K denote the number of different persons (identities) and the number of different images per person, respectively. We perform the experiments with $P = 16$, $K = 4$ using one GPU card. In a batch, the total number of triplets is $T = C_P^N \cdot K^N N(K-1) = 11520$. Even for batch hard mining triplet, the similarities for all the sample pairs in a batch need to be calculated for the selection

Table 2. A case study for combining triplet loss (Tri.) and conventional classification loss (Cls.). *Distance* denotes the similarity metric used for triplet loss. *HardMine* denotes whether batch hard mining is used in triplet loss.

Loss	Distance	HardMine	CUHK03(L)		Market1501		DukeMTMC		MSMT17	
			Rank-1	mAP	Rank-1	mAP	Rank-1	mAP	Rank-1	mAP
Cls.	-	-	67.2	63.6	94.1	83.5	85.6	73.8	72.7	46.8
Tri.	Euclidean	yes	79.4	75.0	94.0	84.8	86.9	74.6	73.8	49.8
Tri.	Euclidean	no	63.7	60.2	87.6	74.0	75.9	59.0	55.0	33.0
Tri.	Cosine	yes	63.3	57.5	83.1	65.3	81.6	66.4	33.2	25.6
Tri.	Cosine	no	43.1	40.6	68.8	50.2	65.0	46.2	25.2	12.5
Tri. + Cls.	Euclidean	yes	79.6	75.8	94.9	86.6	87.3	76.7	78.8	56.0
Tri. + Cls.	Euclidean	no	74.3	70.6	95.0	86.9	87.3	77.1	77.6	53.9
Tri. + Cls.	Cosine	yes	80.7	76.4	94.6	86.9	88.8	77.9	78.6	54.5
Tri. + Cls.	Cosine	no	81.8	78.2	94.7	87.3	88.7	78.3	79.8	56.2

of the hard triples. Actually, triplet using all the triplets has similar training complexity as triplet with hard mining since the computation complexity for summarizing triplet losses only accounts for a very small portion of the total computation complexity of the entire network. But, as the number of classes increases in N-tuple loss, the total number of tuples increases exponentially which becomes intractable quickly. Therefore sampling of the tuples is desirable to limit the complexity. For fair comparisons, in our experiments we sample T tuples for multi-class subsampling classification.

4.3 Empirical Study of Triplet Loss and Conventional Classification Loss for Person ReID

The joint use of the triplet loss and the conventional classification loss achieves superior performance and is predominant in ReID. The implementation details especially for triplet loss (and their variants) differ significantly. However, there is a lack of comprehensive study on their design choices and effectiveness. We investigate the choices on similarity functions (*i.e.*, Euclidean, cosine similarity), sampling mechanisms (batch hard mining or not), and their combinations. Note that for triplet loss, we use soft-margin triplet (see (4)) which has been demonstrated to be better than triplet with hard margin [13] (we have the similar observations).

Table 2 shows the results. We have the following observations. **1)** The joint use of triplet loss (Tri.) and classification loss (Cls.) achieves much better performance than using only one, even outperforming by 4.8% in mAP on CUHK03(L). Triplet loss optimizes local instances to capture local structure while classification loss is capable of exploring the global information about the data distribution. **2)** When Tri. and Cls. are jointly used, cosine similarity in general significantly outperforms (the negative of) Euclidean distance. Note that in the ReID inference, to exclude the interference of the amplitudes (energies) of sample features, normalization on each sample to have unit energy is generally performed for the matching. Cosine similarity inherently evaluates the correlation of two features with energy normalized and it aligns better with ReID inference. **3)** When Tri. and Cls. are jointly used with cosine similarity for triplet, batch

Table 3. Performance comparisons for triplet loss, multi-class subsampling classification (N-tuplet loss), and our proposed MPN-tuplet loss. *Baseline* refers to our strong baseline (the best one in Table 2). *P2S Tri. + Cls.* refers to the use of point-to-set triplet loss and classification loss.

Loss	# Classes	CUHK03(L)		Market1501		DukeMTMC		MSMT17	
		Rank-1	mAP	Rank-1	mAP	Rank-1	mAP	Rank-1	mAP
Baseline (Tri. + Cls.)	2	81.8	78.2	94.7	87.3	88.9	78.3	79.8	56.2
P2S Tri. + Cls.	2	81.1	77.8	94.8	86.7	88.5	78.1	80.0	55.6
N-tuplet + Cls.	2	81.4	77.7	94.4	87.0	88.9	78.1	79.2	55.7
N-tuplet + Cls.	4	82.1	78.4	94.5	87.2	88.8	78.6	80.0	57.2
N-tuplet + Cls.	8	82.1	78.9	94.5	87.5	89.0	79.0	80.3	57.8
N-tuplet + Cls.	16	82.2	79.1	94.7	87.7	89.4	79.2	80.2	58.1
PN-tuplet + Cls.	16	82.9	79.6	94.8	87.5	89.7	78.8	80.9	58.2
MPN-tuplet + Cls.	16	84.4	80.3	95.3	88.7	89.5	79.7	82.2	60.1
MPN-tuplet + Tri. + Cls.	16	84.6	80.8	96.0	88.7	89.9	80.0	82.7	60.5

hard mining (which selects the hard positive and hard negative samples to form a triple) is inferior to the scheme without hard mining. That may be because the soft-margin enables the optimization of moderate hard triples and easy triples. This phenomena is not observed for the Euclidean distance setting. **4)** Without classification loss which globally provides clustering states, triplet loss alone using cosine similarity suffers from difficulty in optimization and is easy to be trapped to local optimal.

Hereafter, we refer to the scheme (last row) with the best combination of design choices as *Baseline*.

4.4 Effectiveness of Multi-class Subsampling Classification Loss and Our MPN-tuplet Loss

We validate the effectiveness of multi-class subsampling classification and our proposed Meta Prototypical N-tuplet (MPN-tuplet) loss on person ReID. Note that conventional classification loss is always used hereafter in considering its complementary role. Table 3 shows the results. *Baseline* refers to our obtained strong baseline (*i.e.*, the best one in Table. 2), where all the triplets within a batch are used for the optimization. *P2S Tri.* refers to point-to-set triplet loss wherein the prototypes (the average results over all instances of the same class) are taken as the reference nodes. This can reduce the number of triplets for calculating multi-class classification losses within a batch to $B = 64$. We observe that *P2S Tri. + Cls.* is competitive (slightly inferior) to *Baseline* but the number of formed triplets within a batch is smaller.

Effectiveness of Multi-class Subsampling Classification. We investigate the influence of the number of simultaneously considered classes (denoted by # Classes) by increasing N in N-tuplet loss. With the increase of N , the number of possible tuples increases exponentially such that it becomes intractable quickly. For example, for the $N = 8$ case, the number of all possible tuples is $C_P^N \cdot K^N N(K-1) = C_{16}^8 \cdot 4^8 \cdot 24 \approx 2.0 \times 10^{10}$. The number of tuples is too large. We randomly sample M tuples to calculate the losses. For fair comparison among schemes with different number of subsampling classes, we set $M = T$, where T is the number of total triplets in a batch. We denote these schemes as *N-tuplet + Cls.*

In Table 3, we observe that as the number of classes in N -tuple loss increases, the person ReID performance in general increases. When the number of classes increases from 2 to 16, the mAP accuracy is improved by 1.4%, 0.7%, 1.1%, and 2.4% on CUHK03, Market1501, DukeMTMC, and MSMT17, respectively. Note that since the baseline scheme *Baseline* is already very strong with superior performance, our gains on top of it can be considered as significant. This enables the training process to be more consistent with a retrieval-based test. Multi-class subsampling classification allows the simultaneous comparison with more than two classes. Note that the performance of N -tuple + *Cls.* with $N = 2$ is lower than the performance of our *Baseline* (*Tri.*+*Cls.*) because the random sampling in N -tuple loss cannot assure a complete traversal over all triplets even though the sampled number is the same as the number of all triplets.

Effectiveness of Our Proposed MPN-tuplet Loss. Similar to $P2S$ *Tri.*+*Cls.*, we could take the prototype as reference node in the tuples instead of using sample instance. We denote such schemes as PN -tuple + *Cls.*. This can significantly reduce the number of possible tuples to $B \cdot C_P^N$. Taking the extreme $N = 16$ case as an example, the number of all possible tuples is reduced to 64 and we use the 64 tuples to calculate the losses. PN -tuple + *Cls.* achieves similar performance as N -tuple + *Cls.* for $N = 16$.

MPN -tuple+*Cls.* denotes our scheme where a mapping subnet (meta learner) is introduced for obtaining reference nodes. This enables a more general similarity metric for effective feature learning. We can see that MPN -tuple+*Cls.* with $N = 16$ achieves significant improvement over PN -tuple+*Cls.*, i.e., 0.7%, 1.2%, 0.9%, and 1.9% gain in mAP accuracy on those four datasets, respectively. The MPN -tuple loss with $N = 16$ is a middle level loss and the conventional classification loss is a global loss. We found when we combine them with the local-level triplet loss, MPN -tuple+*Tri.*+*Cls.* achieves the best performance. Note that at the initial stage when the network has not been trained well, it is challenging for the meta learner to learn a good model. Thus, we use three-stage training. In the first stage, we train the network with classification loss and PN -tuple loss for 360 epoches. In the second stage (361-480 epoches), we fix the network and only train the meta-learner with MPN -tuple loss and the FC layer corresponding to the classification loss. In the third stage (480-600 epoches), we jointly finetune the entire network.

Note that we fix the batch size for fair comparison and convincing ablation study because the learning for person ReID is sensitive to the used batch size. Thus, the number of classes is also limited. We set it to 16. Please see Supplementary for more experimental results.

4.5 Comparison with the State-of-the-Arts

Table 4 shows the comparison with the state-of-the-art approaches. We group these approaches into two groups. The first group aims at designing strong baseline networks, including loss designs and training tricks. In [27], bag of tricks are collected and evaluated for person ReID and a strong baseline built based on ResNet-50 is provided. The other group of approaches focuses on special network designs for ReID. To capture local discriminative information for effective ReID, some approaches [40,48,4] ensemble the local region feature representations. MGN [48] concatenates the feature representations from multiple granularities and achieves good performance. Some approaches

Table 4. Performance (%) comparisons with the state of the art methods. Bold numbers denote the best performance and the numbers with underlines denote the second best ones.

Model		Loss	CUHK03(L)		Market1501		DukeMTMC		MSMT17	
			Rank-1	mAP	Rank-1	mAP	Rank-1	mAP	Rank-1	mAP
Loss Study	IDO-Tri [13]	Tri.	-	-	84.9	69.1	-	-	-	-
	P2S [69]	Tri.	-	-	70.7	44.3	-	-	-	-
	HAP2S [54]	Tri.	-	-	84.6	69.4	76.0	60.6	-	-
	CE-FAT [55]	Tri.	-	-	91.4	76.4	80.8	63.1	69.4	39.2
	IDE [63]	Cls.	43.8	38.9	85.3	68.5	73.2	52.8	-	-
	IDO-Cls [56]	Cls.	62.8	56.7	93.9	80.5	-	-	-	-
	Gp-reid [2]	Tri. + Cls.	-	-	92.2	81.2	85.2	72.8	-	-
	Bag of Tricks [27]	Tri. + Cls. + Center	-	-	94.5	85.9	86.4	76.4	-	-
Others	IANet [14]	Cls.	-	-	94.4	83.1	87.1	73.4	75.5	46.8
	PCB+RPP [40]	Cls.	63.7	57.5	93.8	81.6	83.3	69.2	68.2	40.4
	MGN [48]	Tri. + Cls.	68.0	67.4	95.7	86.9	88.7	<u>78.4</u>	-	-
	DSA-reID [57]	Tri. + Cls.	78.9	75.2	95.7	87.6	86.2	74.3	-	-
	SAN [16]	Tri. + Cls. + Recons.	80.1	76.4	96.1	<u>88.0</u>	87.9	75.5	79.2	55.7
	MHN-6(PCB) [4]	Tri. + Cls.	77.2	72.4	95.1	85.0	<u>89.1</u>	77.2	-	-
	BAT-net [9]	Tri. + Cls.	78.6	76.1	95.1	84.7	87.7	77.3	79.5	56.8
	OSNet [68]	Tri. + Cls.	-	-	94.8	84.9	88.6	73.5	78.7	52.9
	RGA-SC [58]	Tri. + Cls.	80.4	76.5	95.8	88.1	86.1	74.9	<u>81.3</u>	<u>56.3</u>
	Mancs [45]	Tri. + Cls. (focal) + Att.	69.0	63.9	93.1	82.3	84.9	71.8	-	-
	JDGL [65]	GAN (Rec. + Adv.) + Cls.	-	-	94.8	86.0	86.6	74.8	77.2	52.3
Ours	Baseline	Tri. + Cls.	<u>81.8</u>	<u>78.2</u>	94.7	87.3	88.7	78.3	79.8	56.2
	UniCls	MPN-tuplet + Tri. + Cls.	84.6	80.8	<u>96.0</u>	88.7	89.9	80.0	82.7	60.5

introduce attention designs to focus on discriminative features while excluding the interference from irrelevant features [45,9,58]. To address the misalignment challenges caused by the diverse viewpoints and poses, some approaches exploit auxiliary semantics (*e.g.*, dense semantics [57,16]) to address the misalignment in person ReID.

Our study belongs to the first group of approaches. Thanks to the re-investigation on triplet loss design choices, we provide a strong baseline *Baseline*, which jointly uses the soft-margin triplet loss (with cosine similarity, without hard mining) and classification loss (see Table 2 about the ablation study). We can see that our *Baseline* achieves high performance, being superior or competitive to the state-of-the-art approaches. We denote our final scheme with the proposed MPN-tuplet loss as *UniCls*. *UniCls* achieves the best mAP accuracy on all these datasets. *UniCls* outperforms *Baseline* by a large margin, achieving **2.6%**, **1.4%**, **1.7%** and **4.3%** gain in mAP accuracy on the four datasets, respectively. Our design is simple yet effective. There is no increase in the computational complexity during the inference. We hope our scheme could serve as a strong baseline for the ReID community and inspire more new designs on losses.

5 Conclusions

For metric learning of person ReID, we rethink the loss designs and reformulate them from a unified classification view. The predominant losses in ReID, like triplet loss and classification loss, are instantiations of this unified formulation. Triplet loss can be considered as a two-class subsampling classification, which optimizes the feature learning to increase the probability of the anchor sample to be classified as the same class as

the positive sample. We found that simultaneous consideration of instances of multiple class, *i.e.*, multi-class subsampling classification, is capable of significantly improving the performance. That is because the comparison with more instances (instead of only two as in triplet) is more aligned with the ReID inference which is a global-scope ranking process. Moreover, we propose a new multi-class subsampling classification loss, *i.e.*, Meta Prototypical N-tuplet (MPN-tuplet) loss, for effective metric learning. Our scheme powered by MPN-tuplet loss achieves the best performance. We hope that in the future the ReID community will build on top of our strong baseline and investigate more new loss designs.

References

1. Ahmed, E., Jones, M., Marks, T.K.: An improved deep learning architecture for person re-identification. In: CVPR. pp. 3908–3916 (2015)
2. Almazan, J., Gajic, B., Murray, N., Larlus, D.: Re-id done right: towards good practices for person re-identification. arXiv preprint arXiv:1801.05339 (2018)
3. Bai, X., Yang, M., Huang, T., Dou, Z., Yu, R., Xu, Y.: Deep-person: Learning discriminative deep features for person re-identification. Pattern Recognition (2020)
4. Chen, B., Deng, W., Hu, J.: Mixed high-order attention network for person re-identification. In: ICCV. pp. 371–381 (2019)
5. Chen, W., Chen, X., Zhang, J., Huang, K.: Beyond triplet loss: a deep quadruplet network for person re-identification. In: CVPR. pp. 403–412 (2017)
6. Cheng, D., Gong, Y., Zhou, S., Wang, J., Zheng, N.: Person re-identification by multi-channel parts-based cnn with improved triplet loss function. In: CVPR. pp. 1335–1344 (2016)
7. Deng, J., Dong, W., Socher, R., Li, L.J., Li, K., Fei-Fei, L.: Imagenet: A large-scale hierarchical image database. In: CVPR (2009)
8. Do, T.T., Tran, T., Reid, I., Kumar, V., Hoang, T., Carneiro, G.: A theoretically sound upper bound on the triplet loss for improving the efficiency of deep distance metric learning. In: CVPR. pp. 10404–10413 (2019)
9. Fang, P., Zhou, J., Roy, S.K., Petersson, L., Harandi, M.: Bilinear attention networks for person retrieval. In: ICCV. pp. 8030–8039 (2019)
10. Hadsell, R., Chopra, S., LeCun, Y.: Dimensionality reduction by learning an invariant mapping. In: CVPR. vol. 2, pp. 1735–1742 (2006)
11. He, K., Zhang, X., Ren, S., Sun, J.: Deep residual learning for image recognition. In: CVPR (2016)
12. He, L., Sun, Z., Zhu, Y., Wang, Y.: Recognizing partial biometric patterns. arXiv preprint arXiv:1810.07399 (2018)
13. Hermans, A., Beyer, L., Leibe, B.: In defense of the triplet loss for person re-identification. arXiv preprint arXiv:1703.07737 (2017)
14. Hou, R., Ma, B., Chang, H., Gu, X., Shan, S., Chen, X.: Interaction-and-aggregation network for person re-identification. In: CVPR. pp. 9317–9326 (2019)
15. Jia, J., Ruan, Q., Hospedales, T.M.: Frustratingly easy person re-identification: Generalizing person re-id in practice. BMVC (2019)
16. Jin, X., Lan, C., Zeng, W., Wei, G., Chen, Z.: Semantics-aligned representation learning for person re-identification. In: AAAI (2020)
17. Kalayeh, M.M., Basaran, E., Gökmen, M., Kamasak, M.E., Shah, M.: Human semantic parsing for person re-identification. In: CVPR. pp. 1062–1071 (2018)
18. Khamis, S., Kuo, C.H., Singh, V.K., Shet, V.D., Davis, L.S.: Joint learning for attribute-consistent person re-identification. In: ECCV. pp. 134–146 (2014)

19. Krizhevsky, A., Sutskever, I., Hinton, G.E.: Imagenet classification with deep convolutional neural networks. In: *NeurIPS*. pp. 1097–1105 (2012)
20. Lawen, H., Ben-Cohen, A., Protter, M., Friedman, I., Zelnik-Manor, L.: Attention network robustification for person reid. *arXiv preprint arXiv:1910.07038* (2019)
21. Li, W., Zhao, R., Xiao, T., Wang, X.: Deepreid: Deep filter pairing neural network for person re-identification. In: *CVPR*. pp. 152–159 (2014)
22. Li, W., Zhu, X., Gong, S.: Person re-identification by deep joint learning of multi-loss classification. *arXiv preprint arXiv:1705.04724* (2017)
23. Li, W., Zhu, X., Gong, S.: Harmonious attention network for person re-identification. In: *CVPR*. pp. 2285–2294 (2018)
24. Liao, S., Hu, Y., Zhu, X., Li, S.Z.: Person re-identification by local maximal occurrence representation and metric learning. In: *CVPR*. pp. 2197–2206 (2015)
25. Lin, Y., Zheng, L., Zheng, Z., Wu, Y., Yang, Y.: Improving person re-identification by attribute and identity learning. *Pattern Recognition* (2019)
26. Lou, Y., Bai, Y., Liu, J., Wang, S., Duan, L.: Veri-wild: A large dataset and a new method for vehicle re-identification in the wild. In: *CVPR*. pp. 3235–3243 (2019)
27. Luo, H., Gu, Y., Liao, X., Lai, S., Jiang, W.: Bag of tricks and a strong baseline for deep person re-identification. In: *CVPR Workshops*. pp. 0–0 (2019)
28. Luo, H., Jiang, W., Zhang, X., Fan, X., Qian, J., Zhang, C.: Alignedreid++: Dynamically matching local information for person re-identification. *Pattern Recognition* **94**, 53–61 (2019)
29. Paisitkriangkrai, S., Shen, C., Van Den Hengel, A.: Learning to rank in person re-identification with metric ensembles. In: *CVPR*. pp. 1846–1855 (2015)
30. Pan, X., Luo, P., Shi, J., Tang, X.: Two at once: Enhancing learning and generalization capacities via ibn-net. In: *ECCV* (2018)
31. Prosser, B.J., Zheng, W.S., Gong, S., Xiang, T., Mary, Q.: Person re-identification by support vector ranking. In: *BMVC*. vol. 2, p. 6 (2010)
32. Qiao, S., Liu, C., Shen, W., Yuille, A.L.: Few-shot image recognition by predicting parameters from activations. In: *CVPR*. pp. 7229–7238 (2018)
33. Ristani, E., Solera, F., Zou, R., Cucchiara, R., Tomasi, C.: Performance measures and a data set for multi-target, multi-camera tracking. In: *ECCV* (2016)
34. Roweis, S., Hinton, G., Salakhutdinov, R.: Neighbourhood component analysis. *NeurIPS* **17**, 513–520 (2004)
35. Snell, J., Swersky, K., Zemel, R.: Prototypical networks for few-shot learning. In: *NeurIPS*. pp. 4077–4087 (2017)
36. Sohn, K.: Improved deep metric learning with multi-class n-pair loss objective. In: *NeurIPS*. pp. 1857–1865 (2016)
37. Song, C., Huang, Y., Ouyang, W., Wang, L.: Mask-guided contrastive attention model for person re-identification. In: *CVPR*. pp. 1179–1188 (2018)
38. Su, C., Li, J., Zhang, S., Xing, J., Gao, W., Tian, Q.: Pose-driven deep convolutional model for person re-identification. In: *ICCV* (2017)
39. Suh, Y., Wang, J., Tang, S., Mei, T., Mu Lee, K.: Part-aligned bilinear representations for person re-identification. In: *ECCV*. pp. 402–419 (2018)
40. Sun, Y., Zheng, L., Yang, Y., Tian, Q., Wang, S.: Beyond part models: Person retrieval with refined part pooling (2018)
41. Sun, Y., Zheng, L., Yang, Y., Tian, Q., Wang, S.: Beyond part models: Person retrieval with refined part pooling (and a strong convolutional baseline). In: *ECCV*. pp. 480–496 (2018)
42. Varior, R.R., Haloi, M., Wang, G.: Gated siamese convolutional neural network architecture for human re-identification. In: *ECCV*. pp. 791–808 (2016)
43. Varior, R.R., Shuai, B., Lu, J., Xu, D., Wang, G.: A siamese long short-term memory architecture for human re-identification. In: *ECCV*. pp. 135–153 (2016)

44. Vinyals, O., Blundell, C., Lillicrap, T., Wierstra, D., et al.: Matching networks for one shot learning. In: NeurIPS. pp. 3630–3638 (2016)
45. Wang, C., Zhang, Q., Huang, C., Liu, W., Wang, X.: Mancs: A multi-task attentional network with curriculum sampling for person re-identification. In: ECCV. pp. 365–381 (2018)
46. Wang, F., Zuo, W., Lin, L., Zhang, D., Zhang, L.: Joint learning of single-image and cross-image representations for person re-identification. In: CVPR. pp. 1288–1296 (2016)
47. Wang, F., Xiang, X., Cheng, J., Yuille, A.L.: Normface: L2 hypersphere embedding for face verification. In: ACM Multimedia. pp. 1041–1049 (2017)
48. Wang, G., Yuan, Y., Chen, X., Li, J., Zhou, X.: Learning discriminative features with multiple granularities for person re-identification. In: ACM Multimedia. pp. 274–282 (2018)
49. Wang, Y., Wang, L., You, Y., Zou, X., Chen, V., Li, S., Huang, G., Hariharan, B., Weinberger, K.Q.: Resource aware person re-identification across multiple resolutions. In: CVPR (2018)
50. Wei, L., Zhang, S., Gao, W., Tian, Q.: Person transfer GAN to bridge domain gap for person re-identification. In: CVPR (2018)
51. Wei, L., Zhang, S., Yao, H., Gao, W., Tian, Q.: Glad: global-local-alignment descriptor for pedestrian retrieval. In: ACM Multimedia. pp. 420–428 (2017)
52. Weinberger, K.Q., Blitzer, J., Saul, L.K.: Distance metric learning for large margin nearest neighbor classification. In: NeurIPS. pp. 1473–1480 (2006)
53. Yao, H., Zhang, S., Hong, R., Zhang, Y., Xu, C., Tian, Q.: Deep representation learning with part loss for person re-identification. TIP **28**(6), 2860–2871 (2019)
54. Yu, R., Dou, Z., Bai, S., Zhang, Z., Xu, Y., Bai, X.: Hard-aware point-to-set deep metric for person re-identification. In: ECCV. pp. 188–204 (2018)
55. Yuan, Y., Chen, W., Yang, Y., Wang, Z.: In defense of the triplet loss again: Learning robust person re-identification with fast approximated triplet loss and label distillation. arXiv preprint arXiv:1912.07863 (2019)
56. Zhai, Y., Guo, X., Lu, Y., Li, H.: In defense of the classification loss for person re-identification. In: CVPR Workshops. pp. 0–0 (2019)
57. Zhang, Z., Lan, C., Zeng, W., Chen, Z.: Densely semantically aligned person re-identification. In: CVPR. pp. 667–676 (2019)
58. Zhang, Z., Lan, C., Zeng, W., Jin, X., Chen, Z.: Relation-aware global attention. arXiv preprint arXiv:1904.02998 (2019)
59. Zhao, H., Tian, M., Sun, S., Shao, J., Yan, J., Yi, S., Wang, X., Tang, X.: Spindle net: Person re-identification with human body region guided feature decomposition and fusion. In: CVPR (2017)
60. Zheng, L., Shen, L., Tian, L., Wang, S., Wang, J., Tian, Q.: Scalable person re-identification: A benchmark. In: ICCV (2015)
61. Zheng, L., Yang, Y., Hauptmann, A.G.: Person re-identification: Past, present and future. arXiv preprint arXiv:1610.02984 (2016)
62. Zheng, L., Yang, Y., Tian, Q.: Sift meets cnn: A decade survey of instance retrieval. TPAMI **40**(5), 1224–1244 (2017)
63. Zheng, L., Zhang, H., Sun, S., Chandraker, M., Yang, Y., Tian, Q.: Person re-identification in the wild. In: CVPR. pp. 1367–1376 (2017)
64. Zheng, W.S., Gong, S., Xiang, T.: Reidentification by relative distance comparison. TPAMI **35**(3), 653–668 (2012)
65. Zheng, Z., Yang, X., Yu, Z., Zheng, L., Yang, Y., Kautz, J.: Joint discriminative and generative learning for person re-identification. In: CVPR. pp. 2138–2147 (2019)
66. Zheng, Z., Zheng, L., Yang, Y.: Unlabeled samples generated by gan improve the person re-identification baseline in vitro. arXiv preprint arXiv:1701.07717 (2017)
67. Zhong, Z., Zheng, L., Cao, D., Li, S.: Re-ranking person re-identification with k-reciprocal encoding. In: CVPR (2017)

18 Z. Zhang, C. Lan, W. Zeng, Z. Chen, S. Chang.

- 68. Zhou, K., Yang, Y., Cavallaro, A., Xiang, T.: Omni-scale feature learning for person re-identification. In: ICCV. pp. 3702–3712 (2019)
- 69. Zhou, S., Wang, J., Wang, J., Gong, Y., Zheng, N.: Point to set similarity based deep feature learning for person re-identification. In: CVPR. pp. 3741–3750 (2017)